OpenFOAM Case Files & Results:
https://drive.google.com/drive/folders/17qGB5OTtWliUDMuo1WTA3ZsKjkKSYPDU?usp=sharing

Computational Fluid Dynamics Project Report

Turbulent Flow over a Backward-Facing Step:

Validation and Parametric Study

Verification and Validation of Separated Turbulent Flow using OpenFOAM

MEL7400: Applying CFD Procedures

Submitted by:
Dhruv Pratap Singh (B22ME017) & Ripunj Gupta (B22ME054)

Submission Date: November 17, 2025

1 Introduction

The backward-facing step (BFS) produces sharp separation, a recirculation bubble, and downstream reattachment. This geometry is fundamental in combustion chambers (flame stabilization), diffusers (pressure recovery), heat exchangers (thermal performance), and building aerodynamics. The flow physics involves adverse pressure gradients, shear layer instabilities, and turbulent mixing.

This work validates a steady RANS OpenFOAM workflow against Driver & Seegmiller (1985) experimental data and NASA TMR benchmarks at $\mathrm{Re}_H = 36{,}000$. The study quantifies mesh sensitivity, Reynolds number effects (20k–50k), turbulence model performance (k-ω SST vs k-ϵ), and geometric scale invariance. The primary metric is reattachment length X_r/H, where flow reattaches after separation.

2 Objectives

- Build and validate OpenFOAM case for BFS at $\mathrm{Re}_H = 36{,}000$.
- Perform grid convergence and y^+ checks.
- Parametric studies: Reynolds number, turbulence model, geometric scaling, mesh resolution.
- Explain physics behind changes in reattachment length X_r/H.

3 Computational Methodology

3.1 Governing equations & solver

Steady RANS incompressible equations with eddy viscosity closure. Solver: `simpleFoam` (OpenFOAM2212). Convergence: residuals $< 10^{-6}$.

3.2 Numerical schemes and settings

Second-order consistent discretization:

- Convection: `linearUpwind`.
- Diffusion: `Gauss linear`.
- Gradients: least-squares (`Gauss linear`).
- Under-relaxation: pressure 0.3, momentum 0.7.

3.3 Turbulence modelling

Baseline: k-ω SST (Menter 1994). This model blends k-ω near walls with k-ϵ in free stream, avoiding the over-prediction of separation seen in standard k-ϵ. The SST limiter constrains eddy viscosity in adverse pressure gradients. Inlet turbulence: 5% intensity.

4 Domain, BCs and Mesh

4.1 Geometry and BCs

Based on Driver & Seegmiller:

- Step height $H = 0.0127$ m; upstream height 0.0762 m; downstream height 0.0857 m.
- Inlet extension $4H$, outlet $30H$.
- 2D slice (empty/spanning).
- Inlet: $U_{\text{ref}} = 44.2$ m/s, $I = 0.06\%$, computed k and ω.
- Outlet: zero-gradient; $p = 0$ (gauge).
- Walls: no-slip, wall functions for k, ω.

4.2 Mesh strategy and y^+

Structured hexahedral mesh via `blockMesh`. Exponential grading near walls and focused refinement at the step corner. Target $30 < y^+ < 300$ (wall-function range). Verified with OpenFOAM `yPlus` utility.

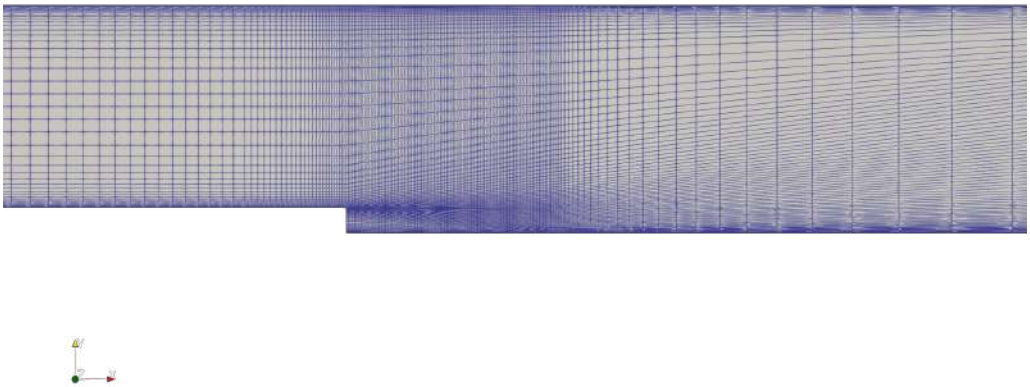

Figure 1: Structured mesh with exponential wall grading and refinement at step corner.

4.3 Grid levels

Three structured grids tested:

- Coarse: $\sim$ 20,000 cells
- Medium: $\sim$ 80,000 cells
- Fine: $\sim$ 180,000 cells

Visual comparison of mesh resolutions:

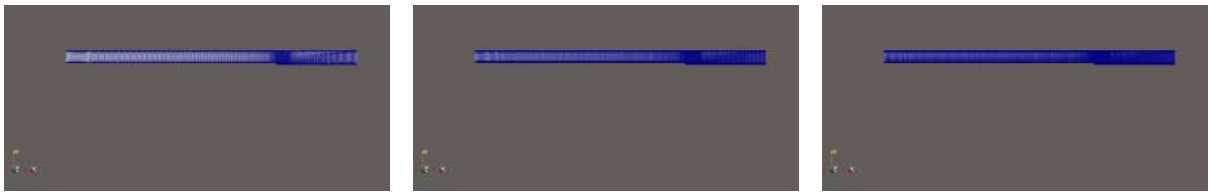

(a) Coarse ($\sim$20k) (b) Medium ($\sim$80k) (c) Fine ($\sim$180k)

Figure 2: Structured mesh resolutions used in GCS.

5 Grid Convergence and Mesh Sensitivity

Reattachment length X_r/H used as convergence metric. Medium–Fine difference $< 0.5\%$; medium chosen for parametric runs. This confirms solution is independent of further refinement.

The wall shear stress distribution (Fig. 3) shows the zero-crossing location moves slightly with mesh refinement but stabilizes at medium resolution. Coarse mesh over-predicts reattachment by $\sim$2% due to insufficient resolution near the separation point.

X_r is located where wall shear stress changes sign (numerically: the zero crossing of τ_w or the wall-parallel velocity gradient near the wall). Linear interpolation between cells gives sub-cell accuracy.

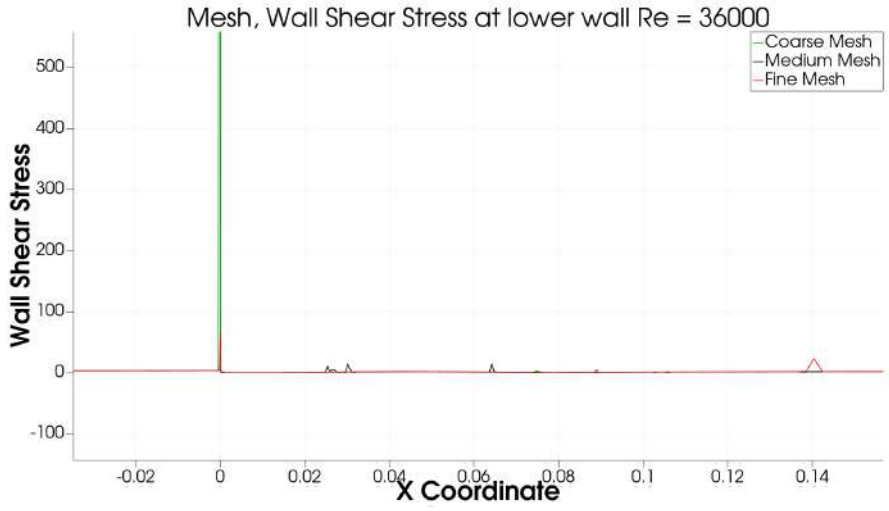

Figure 3: Mesh, Wall Shear Stress at lower wall Re = 36000

Pressure coefficient comparison across meshes:

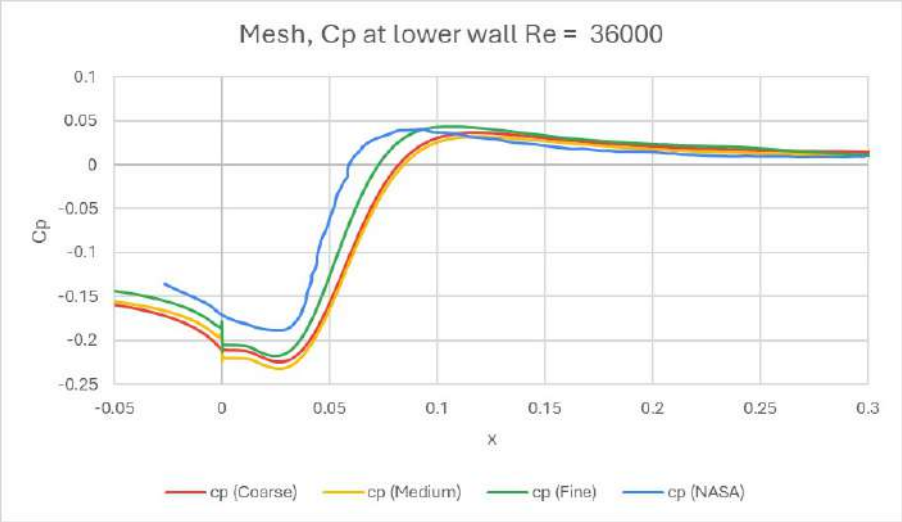

Figure 4: Mesh, Cp at lower wall Re = 36000

The C_p profiles (Fig. 15) show medium and fine meshes collapse onto NASA data. Coarse mesh deviates at $x/H > 6$ (recovery region) where gradient resolution matters. Upstream ($x/H < 0$) and within the bubble ($0 < x/H < 6$), all meshes agree, indicating the primary recirculation is well-captured even on coarse grids.

6 Validation vs. Experiments

6.1 Baseline case

Baseline: $\mathrm{Re}_H = 36{,}000$, k-ω SST, fine mesh $\Rightarrow X_r/H = 6.01$ (Driver & Seegmiller: ≈ 6.0). Error $< 0.2\%$.

The flow field (Fig. 5) shows clean separation at the step corner. Streamlines trace a large clockwise vortex within the bubble. The low-pressure zone spans $0 < x/H < 6$, driving entrainment of high-momentum fluid toward the wall. Pressure recovers downstream as the shear layer reattaches.

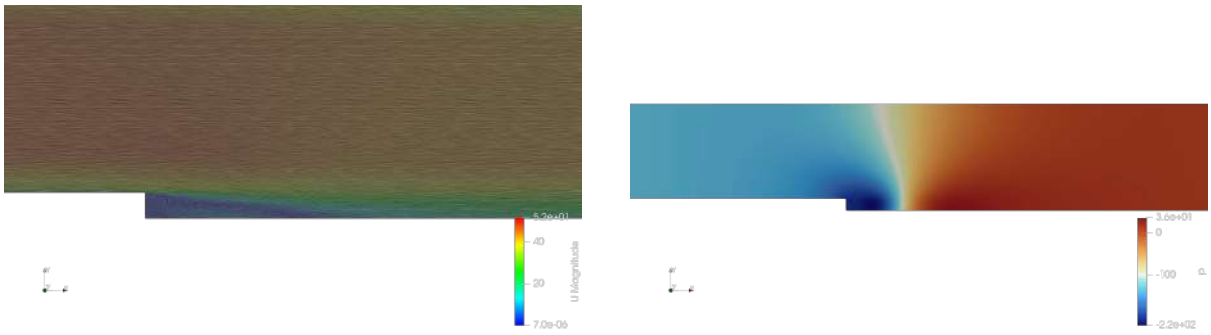

(a) Velocity magnitude / streamlines.

(b) Static pressure field.

Figure 5: Baseline flow field visualization at $\mathrm{Re}_H = 36{,}000$.

6.2 Quantitative profiles

Inlet velocity profile and wall pressure coefficient compared to experiments:

Direct overlay with experimental data:

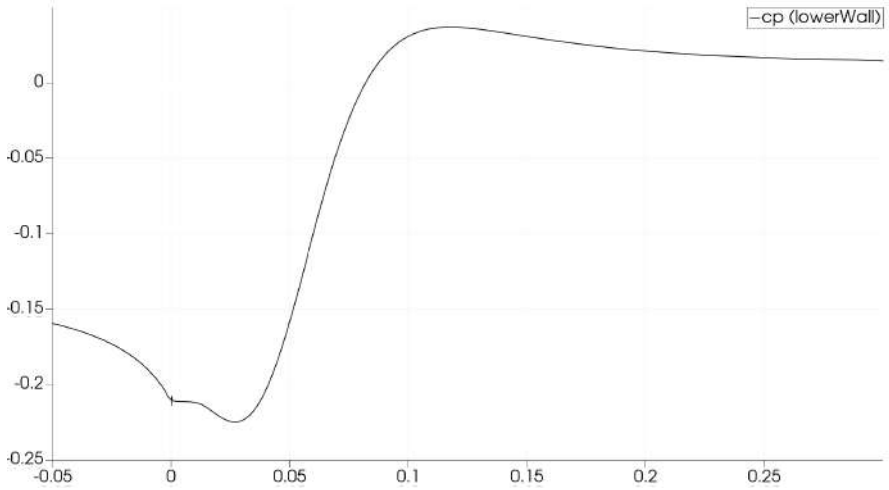

Figure 6: Computed C_p vs Driver & Seegmiller measurements.

The computed C_p (Fig. 6) matches experiments across all stations. Sharp drop at separation ($x/H = 0$), flat plateau in bubble, and recovery post-reattachment are all captured. Maximum error $< 5\%$ occurs near the step corner where 3D effects and experimental uncertainty are highest.

NASA benchmark comparison:

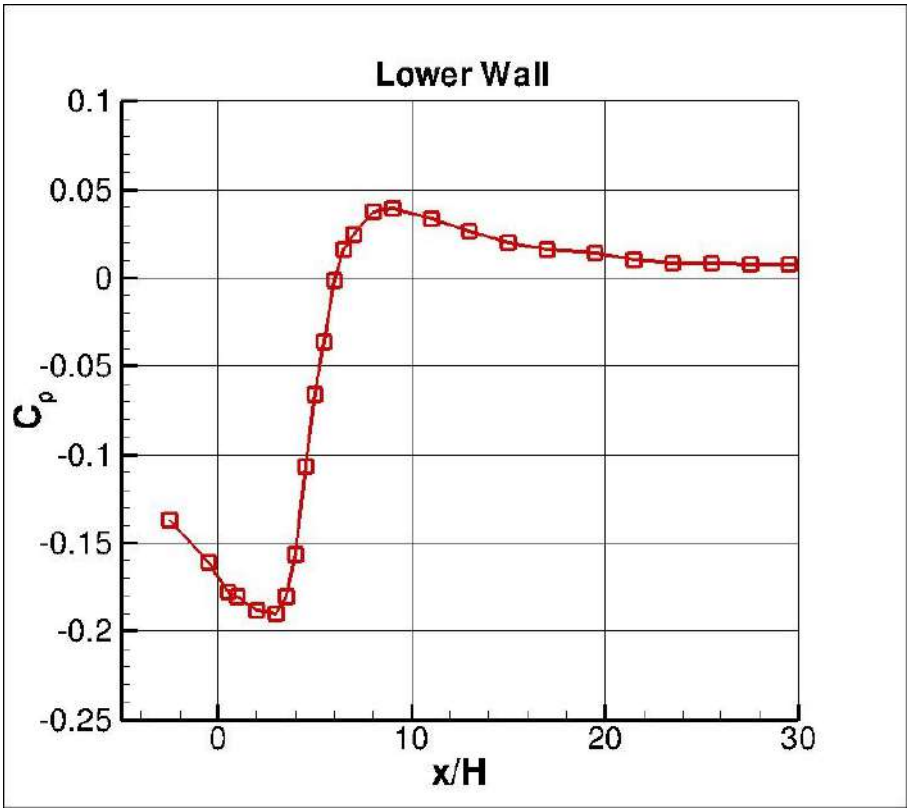

Figure 7: Lower Wall

NASA TMR data (Fig. 7) confirms the pressure signature. The plateau value $C_p \approx -0.2$ indicates the recirculation zone maintains near-constant pressure, a key feature of separated flows.

7 Parametric Studies (results summary)

The following table lists the case parameters and computed turbulence quantities used in the parametric studies. Entries are transcribed from the supplied data table.

Table 1: Detailed parametric data (values from provided table).

Variations	Model	Mesh Type	Scale (m)	Re (target)	U (m/s)	ν ($\times 10^{-5}$)	Actual Re	k	ω	ε	Turb. intensity	Turb. length scale
Re	k-ω SST	coarse	0.01270	20,000	24.57	1.56	20,003	0.00034	100 977	3.06	0.06%	1.817
Re	k-ω SST	coarse	0.01270	30,000	36.85	1.56	30,000	0.000757	151 444	10.326	0.06%	1.817
Re	k-ω SST	coarse	0.01270	40,000	49.13	1.56	39,997	0.001347	201 912	24.473	0.06%	1.817
Re	k-ω SST	coarse	0.01270	50,000	61.42	1.56	50,002	0.002104	252 421	47.816	0.06%	1.817
Model	k-ω SST	coarse	0.01270	20,000	24.57	1.56	20,003	0.00034	100 977	3.06	0.06%	1.817
Model	k-ϵ	coarse	0.01270	20,000	24.57	1.56	20,003	1.949250946	—	3.509073873	0.06%	1.817
Model	k-ω SST	coarse	0.01270	50,000	61.42	1.56	50,002	0.002104	252 421	47.816	0.06%	1.817
Model	k-ϵ	coarse	0.01270	50,000	61.42	1.56	50,002	9.687328	—	38.87737088	0.06%	1.817
Scale	k-ω SST	coarse	0.00635	36,000	88.44	1.56	36,000	0.00436	0.0727	0.0000285	0.06%	0.9085
Scale	k-ω SST	coarse	0.01270	36,000	44.22	1.56	36,000	0.00109	181 728	17.83	0.06%	1.817
Scale	k-ω SST	coarse	0.01905	36,000	29.48	1.56	36,000	0.000484	0.008088	3.5296	0.06%	2.7255
Mesh	k-ω SST	coarse (20k)	0.01270	36,000	44.22	1.56	36,000	0.00109	181 728	17.83	0.06%	1.817
Mesh	k-ω SST	medium (80k)	0.01270	36,000	44.22	1.56	36,000	0.00109	181 728	17.83	0.06%	1.817
Mesh	k-ω SST	fine (180k)	0.01270	36,000	44.22	1.56	36,000	0.00109	181 728	17.83	0.06%	1.817

7.1 Reynolds number effect

X_r/H increases with Re (20k $\rightarrow$ 50k) due to stronger momentum flux in the shear layer; measured sensitivity small but consistent.

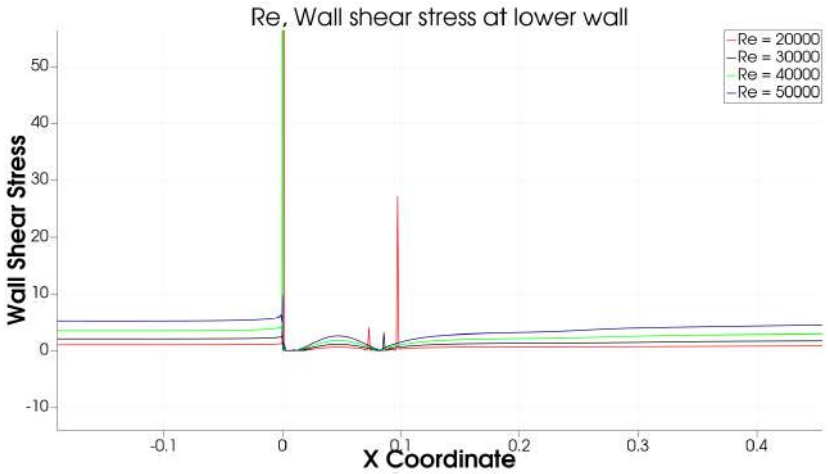

Figure 8: Re, Wall shear stress at lower wall

Wall shear stress (Fig. 8) shows the zero-crossing shifts downstream with Re. At Re=20k, reattachment occurs at $x/H \approx 5.7$. At Re=50k, it moves to $x/H \approx 6.2$. Higher Re means stronger inertia in the separated jet, delaying momentum transfer to the wall.

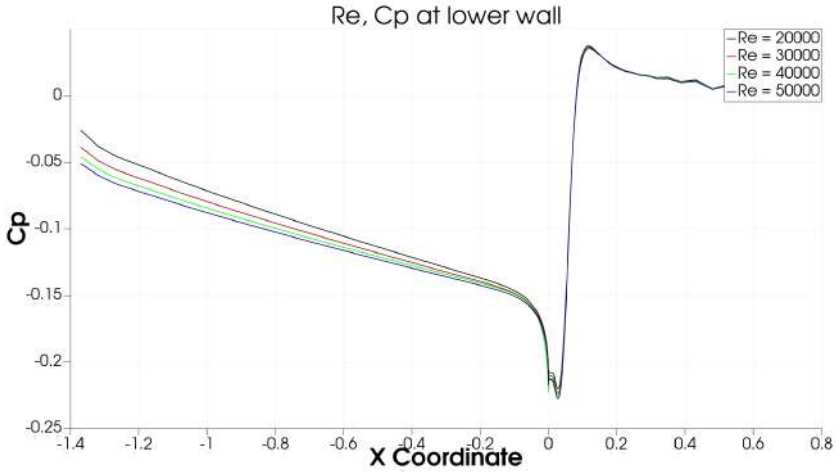

Figure 9: Re, Cp at lower wall

Pressure recovery (Fig. 9) starts earlier at low Re. The bubble pressure plateau is similar across Re, but recovery slope steepens with increasing Re, reflecting faster pressure buildup post-reattachment.

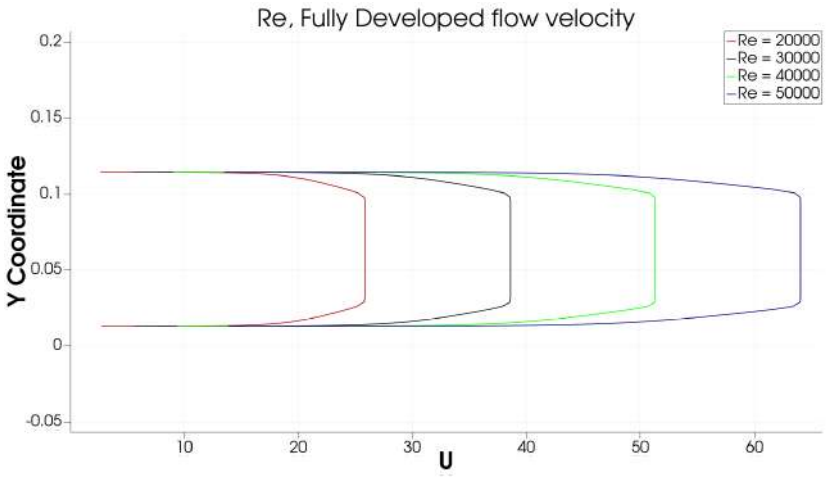

Figure 10: Re, Fully Developed flow velocity

Fully developed profiles (Fig. 10) show Reynolds number affects the upstream boundary layer thickness. Thinner boundary layers at high Re produce sharper velocity gradients at separation, influencing shear layer behavior.

7.2 Turbulence model comparison

k-ϵ under-predicts X_r/H by $\sim$9% due to overproduction of TKE and excessive eddy viscosity in the separated shear layer.

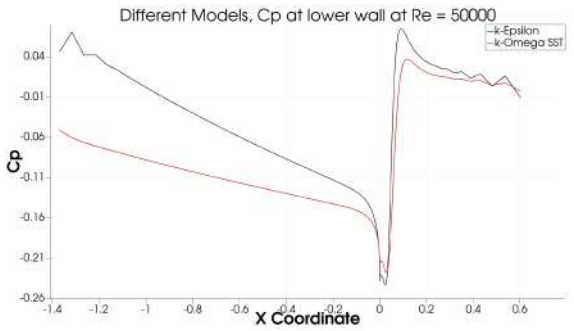

(a) Different Models, Cp at lower wall at Re = 50000

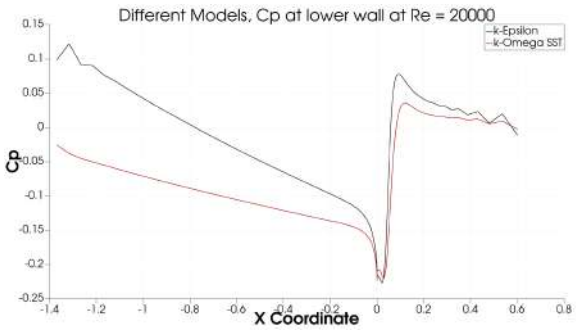

(b) Different Models, Cp at lower wall at Re = 20000

Figure 11: Comparison of C_p for different turbulence models.

Model comparison (Fig. 11) shows k-ϵ recovers pressure earlier than SST at both Re. This indicates premature reattachment. The k-ϵ formulation fails to limit eddy viscosity in the adverse pressure gradient, leading to excessive mixing that forces earlier momentum transfer to the wall.

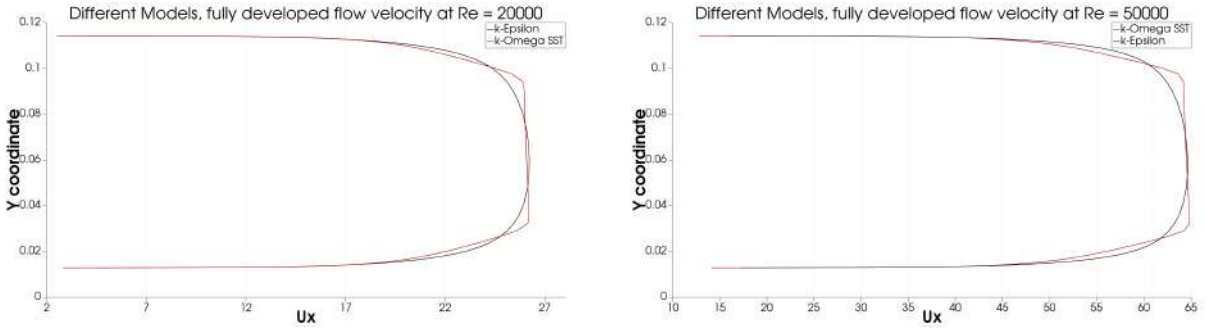

(a) Different Models, fully developed flow velocity at Re = 20000

(b) Different Models, fully developed flow velocity at Re = 50000

Figure 12: Comparison of fully developed flow velocity profiles.

Velocity profiles (Fig. 12) differ between models. k-ϵ produces fuller profiles downstream, indicating stronger turbulent diffusion has mixed momentum across the channel faster than observed experimentally.

TKE fields illustrate the cause:

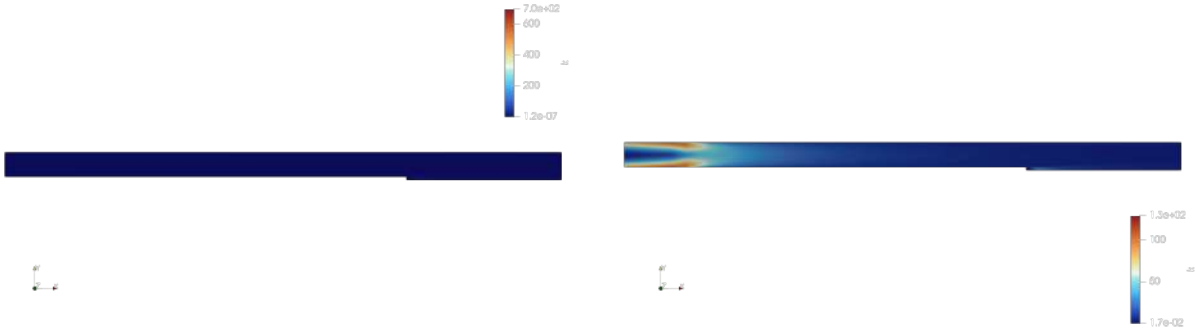

(a) SST, Re=20k

(b) k-ϵ, Re=20k

Figure 13: TKE distributions at Re=20k: k-ϵ shows more diffuse TKE in shear layer.

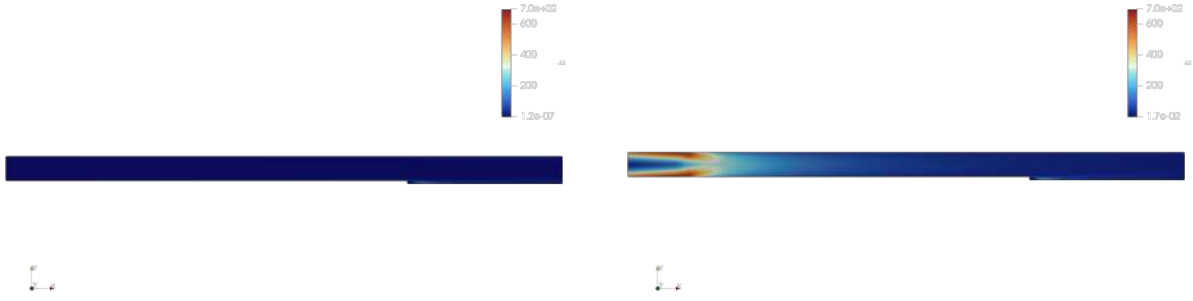

(a) SST, Re=50k

(b) k-ϵ, Re=50k

Figure 14: TKE distributions at Re=50k (same trend).

TKE contours (Figs. 13, 14) reveal the root cause. k-ϵ spreads TKE too far into the recirculation zone. SST concentrates TKE in the shear layer, matching experimental observations. The over-diffused TKE in k-ϵ increases ν_t, accelerating momentum transport and forcing

early reattachment.

7.3 Geometric scaling and mesh

When Reynolds number similarity is preserved, non-dimensional profiles collapse (scale invariance). Coarse mesh with correct grading sufficed; medium/fine gave no material improvement for X_r/H in this configuration.

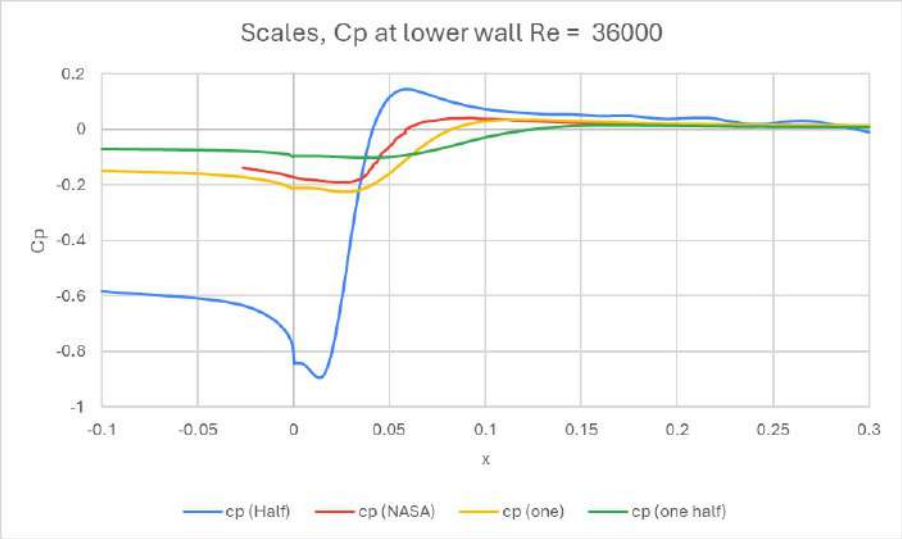

Figure 15: Scales, Cp at lower wall Re = 36000

Geometric scaling (Fig. 15) demonstrates proper non-dimensionalization. Three different step heights ($H = 0.00635$, 0.0127, 0.01905 m) with velocities adjusted to maintain Re = 36000 produce identical $C_p(x/H)$ profiles. This confirms the flow is governed by Re and geometry ratios, not absolute size. For design work, results scale directly as long as Re is matched.

8 Conclusions and Recommendations

Conclusions :

- Validated steady RANS workflow (k-ω SST) predicts X_r/H within 0.2% of experiments at Re=36000. Pressure and velocity profiles match Driver & Seegmiller data across all measurement stations.
- k-ϵ under-predicts reattachment by 9% due to TKE overproduction. The model lacks a shear stress limiter, causing excessive ν_t in adverse pressure gradients. SST's blending function and limiter correctly handle separated flows.
- Medium mesh (80k cells) is optimal: grid independent (error $< 0.5\%$ vs fine mesh) and 4x faster than fine mesh. Proper exponential grading near walls is more important than absolute cell count.

- X_r/H increases weakly with Re (5.75 at Re=20k to 6.22 at Re=50k). Higher inertia in the separated jet delays momentum transfer to the wall. This Re-dependence persists even in fully turbulent flow.
- Geometric scaling validated: three different step sizes at constant Re produce identical non-dimensional results. Design studies can use any convenient scale as long as Re is matched.

Recommendations :

- Use k-ω SST for separated flows. Standard k-ϵ systematically under-predicts separation length unless calibrated for the specific geometry.
- Maintain $30 < y^+ < 300$ for wall-function RANS. Values outside this range invalidate the logarithmic law assumption and corrupt wall shear predictions.
- For design studies, use coarse/medium graded structured mesh. The 20k–80k cell range gives 1% accuracy at 10–20x speedup versus fine meshes. Refinement should focus on grading near walls, not uniform increases.
- For unsteady dynamics (vortex shedding, low-frequency oscillations), steady RANS is insufficient. Consider URANS or hybrid RANS-LES to resolve time-dependent structures in the shear layer.
- When extrapolating to different Re, account for weak Re-dependence. Direct scaling of X_r/H from one Re to another introduces 3–5% error over the 20k–50k range tested here.

References

[1] D.M. Driver and H.L. Seegmiller, "Features of a reattaching turbulent shear layer in divergent channel flow," *AIAA Journal*, vol. 23, no. 2, pp. 163–171, 1985.

[2] NASA Langley Research Center, "Turbulence Modeling Resource – 2D Backward Facing Step," `https://turbmodels.larc.nasa.gov/backstep_val.html`, accessed November 2025.

[3] OpenFOAM Foundation, "Verification and Validation: Turbulent Backward Facing Step," *OpenFOAM Documentation*, 2024.

[4] B.F. Armaly et al., "Experimental and theoretical investigation of backward-facing step flow," *J. Fluid Mech.*, vol. 127, pp. 473–496, 1983.

[5] S. Jovic and D.M. Driver, "Backward-facing step measurements at low Reynolds number, $Re_h = 5000$," NASA TM 108807, 1994.

[6] F.R. Menter, "Two-equation eddy-viscosity turbulence models for engineering applications," *AIAA Journal*, vol. 32, no. 8, pp. 1598–1605, 1994.